A Wireless Respiratory Monitoring System Using a Wearable Patch Sensor Network

Tamer Elfaramawy, Cheikh Latyr Fall, Soodeh Arab, *Student Member, IEEE*, Martin Morissette, François Lellouche, and Benoit Gosselin, *Member, IEEE*

***Abstract*— Wireless body sensors are increasingly used by clinicians and researchers in a wide range of applications, such as sports, space engineering, and medicine. Monitoring vital signs in real time can dramatically increase diagnosis accuracy and enable automatic curing procedures, e.g., detect and stop epilepsy or narcolepsy seizures. Breathing parameters are critical in oxygen therapy, hospital, and ambulatory monitoring, while the assessment of cough severity is essential when dealing with several diseases, such as chronic obstructive pulmonary disease. In this paper, a low-power wireless respiratory monitoring system with cough detection is proposed to measure the breathing rate and the frequency of coughing. This system uses wearable wireless multimodal patch sensors, designed using off-the-shelf components. These wearable sensors use a low-power nine-axis inertial measurement unit to quantify the respiratory movement and a MEMs microphone to record audio signals. Data processing and fusion algorithms are used to calculate the respiratory frequency and the coughing events. The architecture of each wireless patch-sensor is presented. In fact, the results show that the small 26.67 × 65.53 mm^2 patch-sensor consumes around 12–16.2 mA and can last at least 6 h with a miniature 100-mA lithium ion battery. The data processing algorithms, the acquisition, and wireless communication units are described. The proposed network performance is presented for experimental tests with a freely behaving user in parallel with the gold standard respiratory inductance plethysmography.**

***Index Terms*— Breathing rate, coughing detection, inertial measurement unit, wireless, real-time, low-power, wearable, patch sensors network, data fusion.**

I. Introduction

HEALTH care expenses are continuously increasing and are taking a large part of a country's budget. During medical care, vital signs, such as heart and breathing rates, are key parameters that are continuously monitored. Coughing is a prominent indicator of several problems such as chronic obstructive pulmonary disease (COPD), and it is also the main reason for why patients seek medical advice [1]. In fact, it is a pulmonary defense mechanism of the respiratory tract that allows the expulsion of undesirable and irritating substances. Drugman *et al.* [2] studied the performance of several automatic coughing detection sensors and concluded that the best performances are achieved by systems that include an audio microphone which can also be used to measure the breathing activity [3]. In Sleep Disordered Breathing (SDB) studies, the respiratory effort signal is estimated to help in the detection of sleep apnoea [4], [5]. The average typical healthy respiratory rate is around 12 to 20 breaths par minute. In other words, a normal breathing frequency range is around the 0.2 to 0.3 Hz. Several other methods have been used to precisely monitor breathing activity. In-deed, contactless methods exist, like with the Doppler Radar [6]–[8], the ultra-wide band (UWB) radar [9], the laser method [10], using WiFi signals [11], pyro-electric infrared (PIR) sensor [12], a web-cam [13] or with depth images of a Kinect sensor [14], but they aren't suitable for dynamic environments since they usually require a static setup. The respiratory inductance plethysmography (RIP) is presented as the gold standard in breathing surveillance especially for wearable measurement systems [15]. It evaluates pulmonary ventilation by measuring the induction in straps attached around the chest and abdominal wall. Another wearable method is the capacitive sensor as described in [16]. It consists of integrating two textile-based capacitive electrodes on the sides of a shirt which can facilitate long-term monitoring. In [17], the capacitive sensor can be even integrated in a shirt and in [18] six Fiber Bragg grating (FBG) sensors are integrated in a smart textile. Ono *et al.* [19] propose a small piezoelectric sensor placed close to the nose or mouth. It monitors the breathing flow by measuring the temperature and pressure variations. While these solutions can offer precise measurement results with stationary users, they fail with highly mobile users. Additionally, for respiratory and sleep monitoring of freely behaving users, more comfort and unobtrusiveness are needed. Hence, in [20], a respiratory rate system for a stationary user is developed using the three axes of an accelerometer, and in [21], a dynamic respiration monitoring system is obtained from the fusion of an accelerometer with a gyroscope and the use of a Kalman filter, which yielded very compact systems.

In this paper, we present a real time low-power wireless wearable measurement system based on a multimodal patch sensor network that offers unlimited flexibility and mobility

Manuscript received August 20, 2018; revised October 5, 2018; accepted October 5, 2018. Date of publication October 23, 2018; date of current version December 21, 2018. This work was supported in part by the Natural Sciences and Engineering Research Council of Canada, in part by the Fonds de recherche du Québec—Nature et technologies, in part by the Microsystems Strategic Alliance of Quebec, and in part by Oxy'Nov Inc. This is an expanded paper from the IEEE SENSORS 2017 Conference. The associate editor coordinating the review of this paper and approving it for publication was Dr. Rosario Morello. *(Corresponding author: Tamer Elfaramawy.)*

T. Elfaramawy, C. L. Fall, S. Arab, and B. Gosselin are with the Department of Electrical and Computer Engineering, Université Laval, Quebec, QC G1V 0A6, Canada (e-mail: tamer.elfaramawy.1@ulaval.ca).

M. Morissette is with Oxy'Nov Inc., Quebec, QC G2J 0C4, Canada.

F. Lellouche is with the Research Center of IUCPQ, Université Laval, Quebec, QC G1V 0A6, Canada.

Digital Object Identifier 10.1109/JSEN.2018.2877617

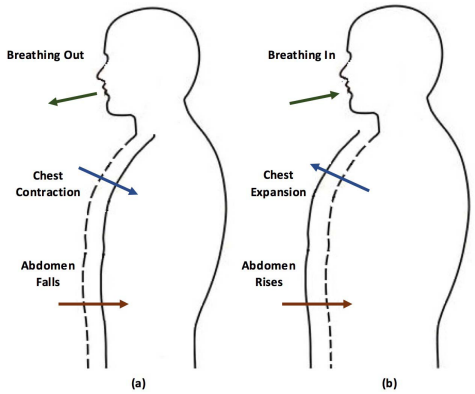

Fig. 1. Representation of the ventral body cavity, made up of the thoracic and abdominal cavities, displacement during expiration (a) and inspiration (b).

for the user. It is designed with a respiratory monitoring system with a coughing detection unit. It uses a complementary filter to fuse the accelerometer and gyroscope data for efficient data processing, it also fuses the data coming from each wireless node and is capable of detecting breathing data while the patient is sitting and walking. In Section II, the system design methodology is explained. In Section III and IV, the hardware and software system design architectures are presented. In Section V, the performance is reported for a freely behaving user before concluding in Section VII.

II. System Overview

While our system was first shown in [22], an in-depth analysis of the system is presented in this paper. The respiratory system consists of all organs involved in breathing including the lungs, all linked blood vessels, the airways such as the nose, the mouth, the larynx, the trachea and the bronchial tubes, and finally the muscles that enable breathing. This system is vital for bringing oxygen into our body that is vital for the survival of our cells and helps eliminating the carbon dioxide, a waste gas, out of the body. The breathing system uses the muscles near the lungs such as the diaphragm, the intercostal, abdominal, neck and collarbone muscles for breathing in a cyclic manner. Hence our methodology consists of measuring the physical movements of the muscles. There are two different types of physical movements during a respiratory cycle, inspiration or breathing in, and expiration or breathing out. The former starts with the intercostal muscles contraction which raises the thoracic cavity and is a joined with the diaphragm lowering. This increases the thoracic intracavity space, decreases its pressure and lets air enter the lungs. The latter continues on with the intercostal muscles bringing the ribcage back in, lowering the thoracic cavity, and with the abdominal muscles raising the diaphragm. The expiration step decreases the thoracic intracavity space while increasing its pressure and letting the air out of the lungs. During this two step respiratory cycle, breathing is expressed through an upper body activity with the thoracic cage, and with a lower body activity with the abdominal cavity because of the important role of the diaphragm and abdominals. Especially during intense physical activities, the entire ventral cavity is compressed and expanded, as seen in Fig. 1. Thus, we use two inertial measurement units (IMU) to measure both the thoracic and abdominal cavity motions simultaneously. Data from both accelerometers and gyroscopes are fused to obtain the breathing rate and photoplethysmographic (PPG) signals in real-time. When a problem arises with the respiratory system, in a case of COPD for instance, the oxygen has difficulty getting processed into the body. A common respiratory symptom used to detect the COPD is coughing which is characterized by a reflex contraction of the breathing muscles and a specific sound. In that regard, a small MEMS microphone is used to record the user's coughing and airway sounds, and to detect its frequency.

III. System Design

A. System Architecture

The overall block diagram of the wireless respiratory monitoring system, presented in Fig. 2, includes two different types of acquisition nodes, one base station and a PC host for data processing, data management and user interaction. The data acquisition node 1, or thoracic node, is equipped with an IMU sensor and a microphone while node 2, or abdominal node, is only equipped with an IMU sensor. These acquisition nodes are responsible for acquiring data from the different sensors. They are placed on the body such as to obtain the abdominal and thoracic breathing activities. Each one is built around a MSP430 low-power microcontroller (MCU) from Texas Instruments and use a LSM9DS0 IMU from STMicroelectronics. Node 1 is also equipped with an analog ADMP401 MEMS microphone from Analog Devices.

B. Microcontroller and Acquisition Nodes

The MSP-EXP430F5529LP, a development kit for the low power MCU MSP430, is used for prototyping the acquisition nodes that process the IMU's and the microphone, as well as for developing the wireless transceiver. As seen in Fig. 2, the 16-bit MSP430F5529 MCU gathers data from the IMU and the microphone before being sent wirelessly to the base-station, using the low-power nRF24L01 radio module from Nordic Semiconductor. In the case of acquisition node 1, after that the analog audio data goes through an anti-aliasing filter at 5 kHz, see Fig. 3, it is sampled at a frequency of 10 kHz using the 12-bit analog-to-digital converter (ADC), then buffered using the direct memory access (DMA). Simultaneously, at a rate of 32 Hz, a serial peripheral interface bus (SPI) is used to transmit data from the IMU to the MCU where it is processed to calculate the thoracic and abdominal displacement angles. Finally, both data, the displacement angles and the audio data, are relayed to the wireless transceiver using an SPI connection.

C. Wireless Transceiver

The low-power nRF24L01 radio module from Nordic Semiconductor, is used for all wireless transmission in the respiratory monitoring system. It transmits data from both acquisition nodes to the base-station where acquired breathing and coughing data are extracted. The RF IC can achieve up to 2 Mbps on-air data rate, has transmission peaks less than 13 mA, offers sub μA idle mode and is supplied on a 3.3 V supply voltage.

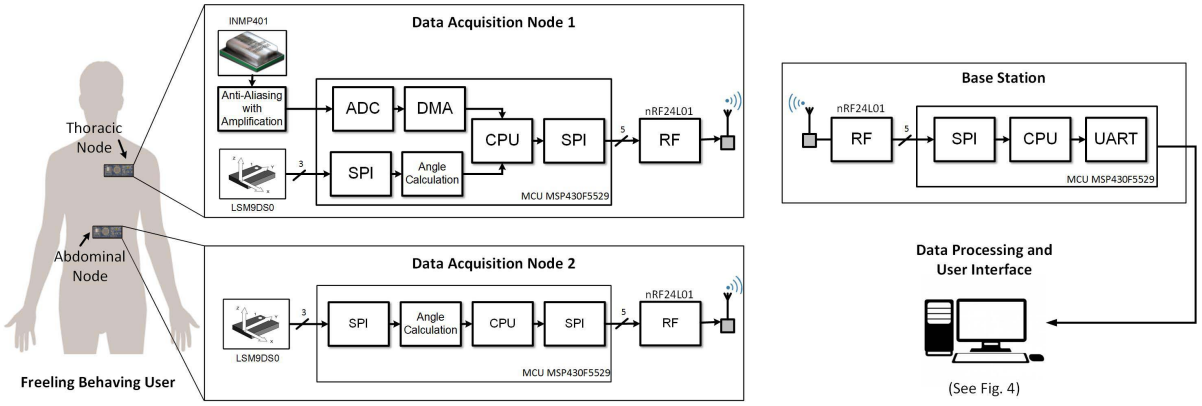

Fig. 2. Block diagram of the proposed wireless body sensor network including the data acquisition nodes, the base station, and, the data processing and user interface.

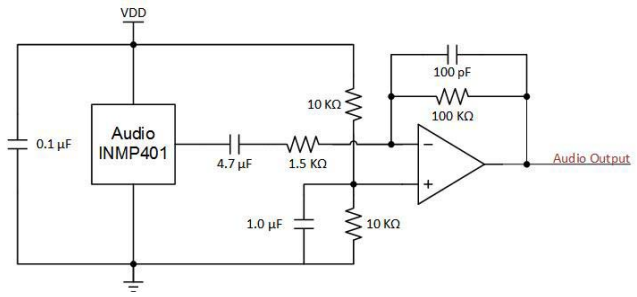

Fig. 3. Circuit schematic of INMP401 analog MEMS microphone.

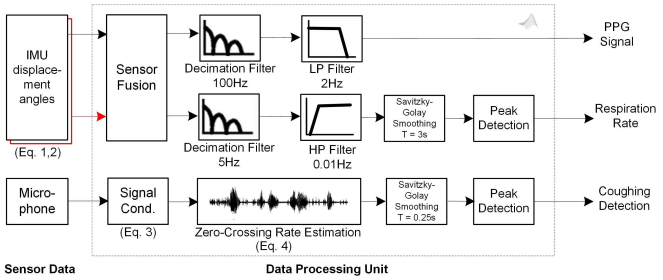

Fig. 4. Block diagram of the signal processing unit including: the respiration rate waveform unit, the respiration rate unit and the coughing detection unit.

IV. Data Processing and Algorithms

While the abdominal and thoracic displacement angles processing are implemented directly within the sensor nodes (in-situ), the signal processing unit, depicted in Fig. 4, is implemented ex-situ, inside the PC host. In fact, through this unit is calculated the breathing frequency and the occurrence of coughing, the details of which calculations are provided in the next sections.

A. User Interface

The user interface as well as the digital signal processing are both developed in MATLAB. The interface allows the user to visualize the motion and the derived PPG and sound signals acquired from the 2 sensor nodes in real-time. Fig. 5 is a caption of the MATLAB interface that shows the displacement of the ventral body cavity corresponding to PPG signal (Fig. 5(a)), and the audio output of the microphone (Fig. 5(b)). The respiratory frequency and the coughing occurrence are depicted as well.

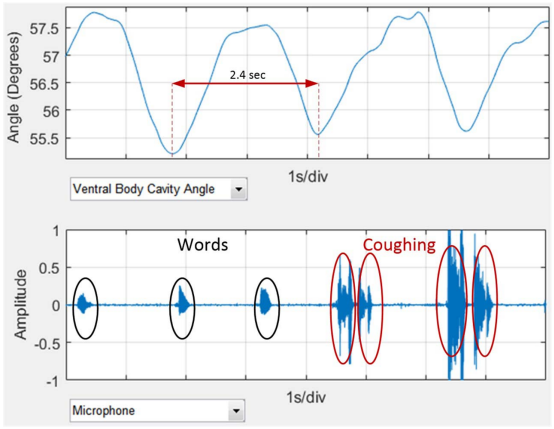

Fig. 5. Screenshot of the user interface showing the PPG (top) and the audio signal showing speech (in black circles) and coughing (in red circles).

B. Abdominal and Thoracic Displacement Angles

Within the sensor nodes, the IMU provides the accelerometer and gyroscope data to the MCU through an SPI interface bus. To achieve a high speed transfer rate between the sensor nodes and the base station, the amount of data to be transmitted wirelessly is reduced through data processing in each node. In fact, among the axes offered by the IMU, are 3 acceleration axes and 3 rotational motion axes needed to calculate the displacement angles. Instead of sending 6 data channels to the base station, an interrupt routine is executed at a frequency of 32 Hz within the nodes, where the abdominal and thoracic displacement angles (or IMU rotation angles) are calculated thanks to a first order complementary filter as show in Fig. 6, and then sent with the rest of data. Below, (1) and (2) are used to calculate the angles when a user is standing or walking. ω_x is the rotational velocity along the x-vector, a_y and a_x are the acceleration components along the y and x-vector,

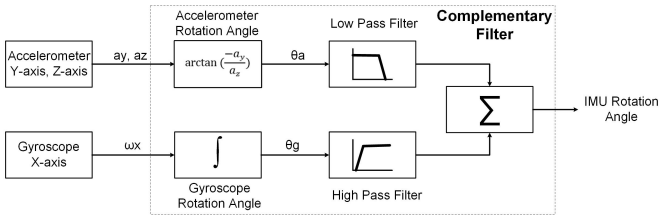

Fig. 6. Block diagram of the complementary filter used to calculate the abdominal and thoracic displacement angles where ay and az are the acceleration components on the y and z-vector, ω_x the rotational velocity along the x-vector, θ_a the accelerometer rotation angle and θ_g the gyroscope rotation angle.

angle is the displacement angle, α_{gyro} and α_{acc} are the complementary filter coefficients. In Fig. 6, α_{gyro} and α_{acc} are represented by low and high pass filters. In-deed, $\alpha_{acc}.\theta_a[n]$ acts the low pass filtering of the accelerometer rotation angle while $\alpha_{gyro}.\ \theta_g[n]$ represents the high pass filtering of the gyroscope rotation angle. In other words, the complementary filter calculates a rotation angle around a desired vector by removing noise from the accelerometer, eliminating the gyro drift and by fusion them.

$$angle[n] = \alpha_{gyro}.\theta_g[n] + \alpha_{acc}.\theta_a[n] \tag{1}$$

with

$$\begin{cases} \alpha_{gyro} = 1 - \alpha_{acc} \\ \theta_g[n] = angle[n-1] + \omega_x[n].\Delta t \\ \theta_a[n] = atan2(-a_y, a_z) \end{cases} \tag{2}$$

When the user is laying down, different vectors are used. The optimal vectors are decided by comparing them to the gravitational vector such as no disruptions occur when calculating the rotational angle during the respiration cycle since the angle is limited to $-\frac{\pi}{2}$ and $\frac{\pi}{2}$.

C. Breathing Activity

Breathing activity is expressed from the chest and abdomen. Hence, after initial synchronization of data coming from each node, a data fusion is performed by calculating the arithmetic mean of both, the abdominal and thoracic displacements angles, to achieve a ventral body cavity angle. To obtain the real-time PPG, only a few steps are needed. First the average displacement angle is calculated over a 3-second window and eliminated to remove the body movement, then a 20th order low-pass FIR filter with a cut-off frequency at 2 Hz is used. For the respiration rate, several steps are needed to ensure that all high-frequency components are eliminated, but also all noise artifacts coming from the body. Especially since the calculated ventral cavity angle includes the breathing movement, but also any rotation around the sensor node like body movements. Hence, the ventral cavity angle is decimated to 5 Hz to eliminate all high frequency components and followed by a 1st order high-pass filter at 0.01 Hz to remove the baseline wander. A Savitzky-Golay smoothing filter, chosen for its easy and efficient implementation in many systems including in [21], is used to smooth the signal before applying a peak detection algorithm to detect the breathing peaks. In Fig. 7(a) and (b), the signal is presented before and after its filtering and peak detection.

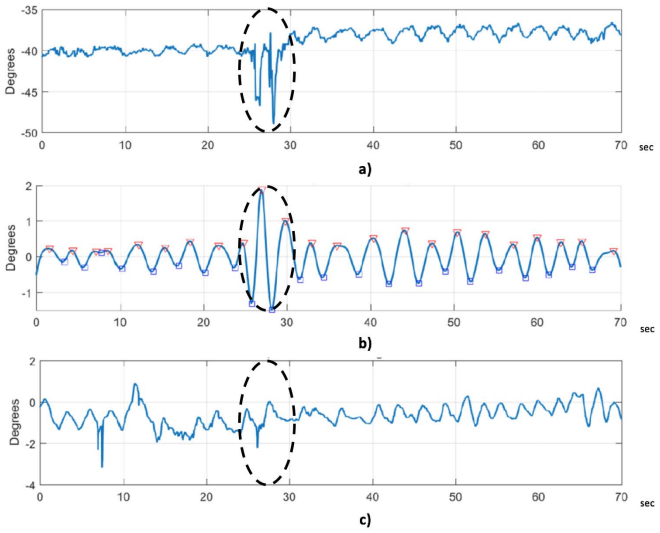

Fig. 7. The ventral body cavity angle before (a) and after (b) signal processing, and (c) the RIP signal as a reference, with a distortion circled in black.

D. Cough Detection

To detect coughing, we propose a simple but efficient method. Audio data is usually sampled at a high frequency of 10 kHz. In the MCU, to ensure that the data is transferred without interrupting other tasks, a DMA is used. After data synchronization, two seconds of audio data is saved for processing. The zero-crossing rate (ZCR), which is heavily used in speech recognition, is taken as the sign change rate along the recorded audio signal [23]. Here, it is used to detect the strong important signal changes when coughing occurs. Furthermore, to maximize the algorithm efficiency, noise floor is eliminated by setting to zero all data smaller than a predetermined threshold coefficient Γ, as seen in (3).

$$S[n] = \begin{cases} S[n], & \text{if } S[n] > \Gamma \\ 0, & \text{if } S[n] < \Gamma \end{cases} \tag{3}$$

The ZCR is then applied, as seen in (4), where S is the signal of length T and $1_{\Re_{<0}}$ the indicator function.

$$zcr = \frac{1}{T-1} \sum_{t=1}^{T-1} 1_{\Re_{<0}}(S_t S_{t-1} < 0) \tag{4}$$

Hence, to differentiate coughing from speech, a peak detection algorithm is applied following a Savitzky-Golay smoothing filter to detect only events with a higher zero-crossing rate.

V. Measured Performances

In this section, we look at the wireless monitoring wearable sensor performances in terms of durability, autonomy, usability and precision. The final wireless respiration monitoring system characteristics and measurements are shown in Table I.

TABLE I
SUMMARY OF SYSTEM CHARACTERISTICS

Parameters	Value
ISM Band	2.4 GHz
RF Range	8 m
Microphone SNR	62 dBA
IMU data output	16-bit
Supply Voltage	3.7 V
Current Consumption for abdominal node	12 mA
Current Consumption for thoracic node	16.2 mA
Life Span 100 mA lithium battery	6 hours
PCB Dimensions	26.67 x 65.53 mm^2

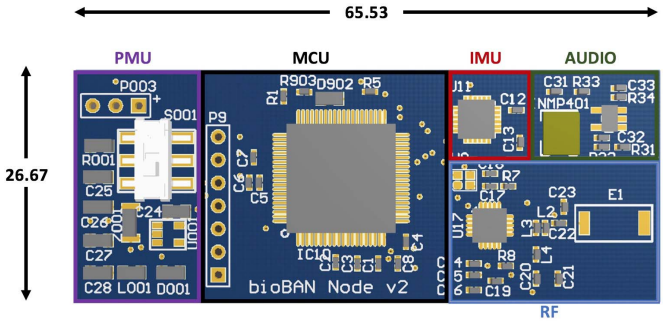

Fig. 8. Printed circuit board of the proposed multimodal patch sensor.

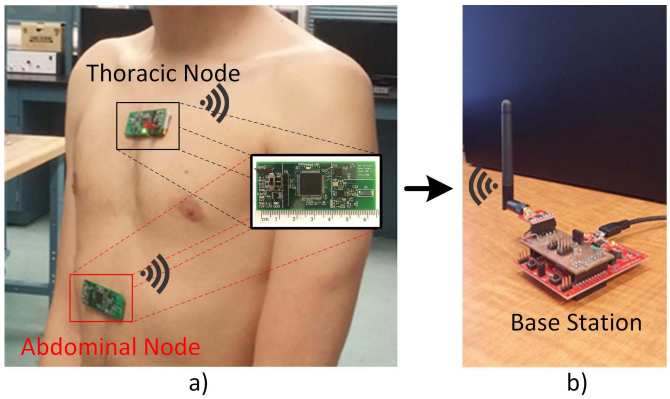

Fig. 9. Picture of the 2 sensor nodes (node 1 in black and node 2 in red) placed on user (left) and base station (right).

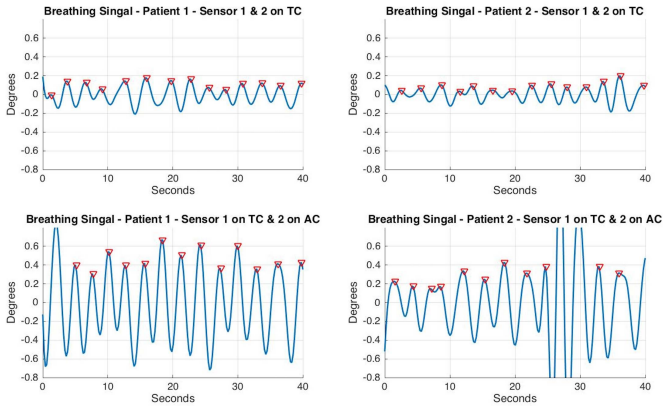

Fig. 10. The ventral body cavity angle after signal processing, also named Filtered Roll, for 2 different users when the sensors are both placed on the thoracic cavity (or TC) and when 1 is placed on the thoracic cavity and the other on the abdominal cavity (or AC).

A. Multimodal Patch Sensor

The wireless respiratory monitoring and coughing detection sensor network is composed of two nodes. Each node is designed using a 4-layer printed circuit board, including 2 signal layers, 1 ground layer and 1 supply voltage layer, as seen in Fig. 8. The boards measures 26.67 × 65.53 mm^2 which is big enough to enable a programming input port identified by *P9* and small enough to be carried easily and flexibly by the user. The minimum gap between tracks is 0.2 mm and the holes minimum diameter is 0.4 mm. The printed circuit board is composed of 5 main units including the microcontroller unit (MCU), the power management unit (PMU), the inertial measurement unit (IMU), the audio unit (AUDIO) and the radio frequency module (RF), as seen in Fig. 8. The sensor is powered with a 3.7-V 100-mAh Li-ion battery and its RF-link allows up to 8 meters of transmission.

B. Experimentation Procedures

During the experimentation, a user had the two sensor nodes placed on the thoracic and abdominal cage, see Fig. 9, and in the same time, a medical respiratory inductance plethysmography (RIP) belt was attached around the chest as a reference. Firstly, several experimental tests were done to find the optimal sensors location. Secondly, a performance test was done while the user was walking to demonstrate its robustness. Finally, the proposed monitoring system's performance is compared to the RIP belt.

C. Respiration Signal Analysis

An experimental test was performed to study the difference in breathing signal results when the sensor is placed on the thoracic and the abdominal cage. In Fig. 10, a comparison of the breathing signal coming from two users when the sensors are both placed on the thoracic cage and when each is placed on the abdominal and the thoracic cavity. It can clearly be seen that when one of the sensors is placed on the abdominal cavity, the amplitude of the signal is greatly enhanced. This is due to the fact that when sitting the users breaths mostly from the abdominal area whereas when the user is doing a physical exercise, the breathing will be enhanced in the thoracic area. In Fig. 11, the robustness was demonstrated by having the user test the monitoring system while sitting and walking. In fact, at the 25th second of the *Angle Fusion while walking* signal, noise coming from the movement is filtered to obtain a breathing cycle as seen in the second signal *Filtered Angle During walking*. During the third experimental test, the breathing cycles obtained through the medical gold standard RIP belt and from our wireless monitoring system were compared

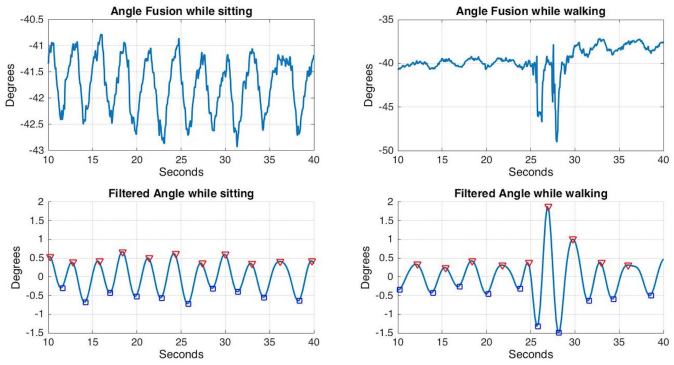

Fig. 11. The ventral body cavity angle before (a) and after (b) signal processing when the user is sitting and walking.

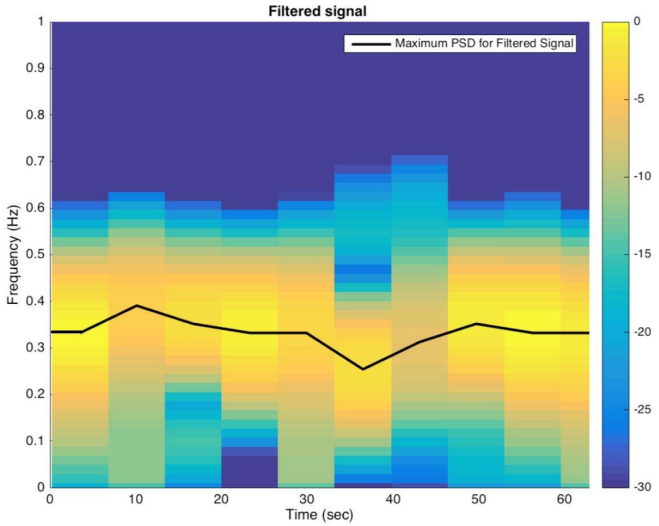

Fig. 12. The spectrogram of a 60 second processed breathing signal sample with the maximum PSD shown in black.

as shown in Fig. 7. In the latter, the angle before and after filtering, and the RIP signal are all shown while the user is walking. The figure particularly shows the system functioning correctly while the user is moving. Furthermore, it is able to detect breathing patterns during heavy distortions as seen circled in black at the 25th second in the three graphs, where the user disrupts the signal by sneezing. Also, a significant synchronization time was needed for each new use when setting the RIP belt up while data from the patch was obtained almost instantaneously. Finally, the spectrogram of a processed respiratory signal, presented in Fig. 12, shows its maximum PSD during 60 seconds of breathing. In this figure, the signal power is clearly concentrated between 0.2 and 0.4 Hz with the maximum power at around 0.35 Hz. In fact, the PPG of this signal shows around 23 breathing cycles during 60 seconds, which corresponds to around 0.38 Hz. The signal analysis through the spectrogram is an important tool in understanding the breathing signal distribution through time as well as for building the respiratory data processing algorithms.

D. Power Consumption

While the abdominal sensor node consumes only 12 mA, the thoracic sensor node consumption goes up to 16.2 mA with a 3.7 V supply voltage because of a higher data transmission rate due to the microphone. In Fig. 13, the consumption breakdown for the latter is shown.

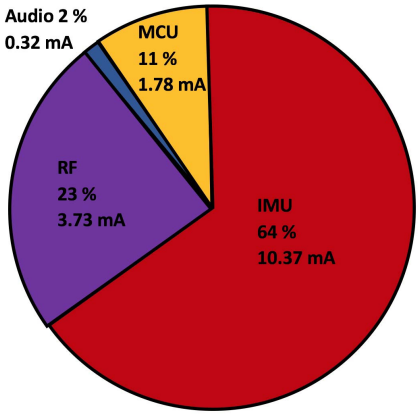

Fig. 13. Power consumption breakdown of the sensor nodes in %.

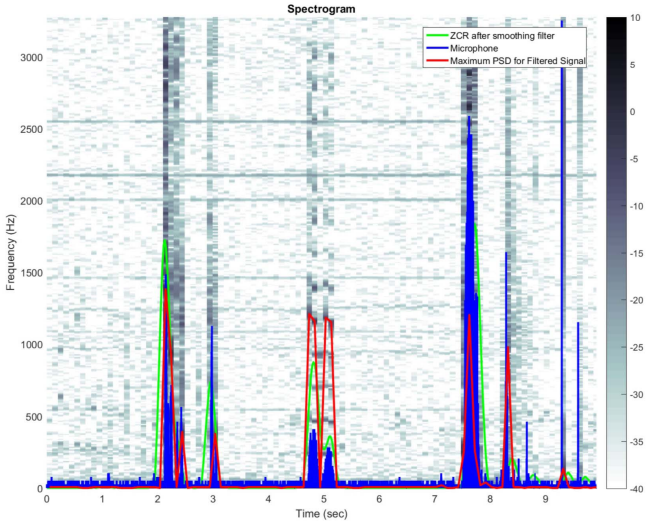

Fig. 14. The microphone audio signal spectrogram showing coughing events with the audio microphone signal in blue, the filtered ZCR of the signal in green and maximum PSD of the filtered signal in red.

E. Coughing Detection

In Fig. 5, an image of the interface showing the PPG signal and the audio signal is given. In the latter, the coughing events and the pronunciation of words can be discriminated in the audio signal. Indeed, the ZCR was able to differentiate between the different audio sounds and recognize a cough. In Fig. 14, a spectrogram of the microphone audio signal shows the correlation between the maximum PSD of the audio signal, shown in red, and the zero-crossing rate, show in green. In blue, the original audio signal is shown with several signal peaks corresponding to coughing events. In fact, these important signal variations that occur when the user is coughing, distinct by a strong power spectral density, are detected with a simple but efficient algorithm. Thanks to a

peak detection algorithm applied on the filtered ZCR signal, every coughing event can be easily identified.

VI. Discussion

The breathing activity analysis including the respiratory frequency, the photoplethysmogram with the detection of each cough event are all important respiratory parameters that can help in the development of a robust and reliable diagnosis and monitoring technologies. Hence, the next step will consist of fusing respiratory and coughing data for a complete modeling and analysis of the respiratory system. Further studies would also include its application in the clinical assessment of breathing activities and of cough.

VII. Conclusion

A real-time wireless respiratory monitoring system with coughing detection is presented for patient surveillance during ambulatory, hospital and home care. It uses low-power electronic building blocks and is designed to maximize the movement and comfort for the user with its small size circuit, see Table I. Its set-up is much quicker and easier to use than the RIP used in hospitals since it doesn't need any synchronization. Results show that the system can acquire breathing data while the patients is resting but also when walking. While the system is able to detect the coughing occurrence, more complex algorithms have been proposed in speech recognition that can be used to improve its efficiency especially when talking [2], [23]. The MCU and RF module power consumption can be greatly improved through ASIC design. The system can also be expanded to include cardiovascular, blood pressure and temperature monitoring units to increase diagnostic reliability. Future work will also include developing more robust algorithms to enable continuous breathing surveillance during different sports activity.

References

[1] S. M. Schappert and C. W. Burt, "Ambulatory care visits to physician offices, hospital outpatient departments, and emergency departments: United States, 2001–02," *Vital Health Statist. Ser. Data Nat. Health Surv.*, vol. 159, pp. 1–66, Feb. 2006.

[2] T. Drugman *et al.*, "Objective study of sensor relevance for automatic cough detection," *IEEE J. Biomed. Health Inform.*, vol. 17, no. 3, pp. 699–707, May 2013.

[3] Y. Nam, B. A. Reyes, and K. H. Chon, "Estimation of respiratory rates using the built-in microphone of a smartphone or headset," *IEEE J. Biomed. Health Inform.*, vol. 20, no. 6, pp. 1493–1501, Nov. 2016.

[4] M. Jayawardhana and P. de Chazal, "Enhanced detection of sleep apnoea using heart-rate, respiration effort and oxygen saturation derived from a photoplethysmography sensor," in *Proc. 39th Annu. Int. Conf. IEEE Eng. Med. Biol. Soc. (EMBC)*, Jul. 2017, pp. 121–124.

[5] I. Sadek, E. Seet, J. Biswas, B. Abdulrazak, and M. Mokhtari, "Non-intrusive vital signs monitoring for sleep apnea patients: A preliminary study," *IEEE Access*, vol. 6, pp. 2506–2514, 2018.

[6] X. Gao, A. Singh, E. Yavari, V. Lubecke, and O. Boric-Lubecke, "Non-contact displacement estimation using Doppler radar," in *Proc. Annu. Int. Conf. IEEE Eng. Med. Biol. Soc. (EMBC)*, Aug./Sep. 2012, pp. 1602–1605.

[7] W. Li, B. Tan, and R. J. Piechocki, "Non-contact breathing detection using passive radar," in *Proc. IEEE Int. Conf. Commun. (ICC)*, May 2016, pp. 1–6.

[8] A. Üncü, "A 24-GHz Doppler sensor system for cardiorespiratory monitoring," in *Proc. 42nd Annu. Conf. IEEE Ind. Electron. Soc. (IECON)*, Oct. 2016, pp. 5161–5164.

[9] Q. Jian, J. Yang, Y. Yu, P. Björkholm, and T. McKelvey, "Detection of breathing and heartbeat by using a simple UWB radar system," in *Proc. 8th Eur. Conf. Antennas Propag. (EuCAP)*, Apr. 2014, pp. 3078–3081.

[10] T. Kondo, T. Uhlig, P. Pemberton, and P. D. Sly, "Laser monitoring of chest wall displacement," *Eur. Respirat. J.*, vol. 10, no. 8, pp. 1865–1869, 1997.

[11] S. Lee, Y.-D. Park, Y.-J. Suh, and S. Jeon, "Design and implementation of monitoring system for breathing and heart rate pattern using WiFi signals," in *Proc. 15th IEEE Annu. Consum. Commun. Netw. Conf. (CCNC)*, Jan. 2018, pp. 1–7.

[12] F. Erden and A. E. Cetin, "Breathing detection based on the topological features of IR sensor and accelerometer signals," in *Proc. 50th Asilomar Conf. Signals, Syst. Comput.*, Nov. 2016, pp. 1763–1767.

[13] T. Nochino, Y. Ohno, and S. Okada, "Development of noncontact respiration monitoring method with Web-camera during sleep," in *Proc. IEEE 6th Global Conf. Consum. Electron. (GCCE)*, Oct. 2017, pp. 1–2.

[14] T. Ushijima and J. Satake, "Development of a breathing detection robot for a monitoring system," in *Proc. Joint 8th Int. Conf. Soft Comput. Intell. Syst. (SCIS), 17th Int. Symp. Adv. Intell. Syst. (ISIS)*, Aug. 2016, pp. 790–795.

[15] A. Hart, K. Tallevi, D. Wickland, R. E. Kearney, and J. A. Cafazzo, "A contact-free respiration monitor for smart bed and ambulatory monitoring applications," in *Proc. Annu. Int. Conf. IEEE Eng. Med. Biol.*, Aug./Sep. 2010, pp. 927–930.

[16] S. K. Kundu, S. Kumagai, and M. Sasaki, "A wearable capacitive sensor for monitoring human respiratory rate," *Jpn. J. Appl. Phys.*, vol. 52, no. 4S, p. 04CL05, 2013. [Online]. Available: http://stacks.iop.org/1347-4065/52/i=4S/a=04CL05

[17] S. W. Park, P. S. Das, A. Chhetry, and J. Y. Park, "A flexible capacitive pressure sensor for wearable respiration monitoring system," *IEEE Sensors J.*, vol. 17, no. 20, pp. 6558–6564, Oct. 2017.

[18] D. L. Presti *et al.*, "Respiratory and cardiac rates monitoring during MR examination by a sensorized smart textile," in *Proc. IEEE Int. Instrum. Meas. Technol. Conf. (I2MTC)*, May 2017, pp. 1–6.

[19] Y. Ono, D. Mohamed, M. Kobayashi, and C.-K. Jen, "Piezoelectric membrane sensor and technique for breathing monitoring," in *Proc. IEEE Ultrason. Symp.*, Nov. 2008, pp. 795–798.

[20] A. Bates, M. J. Ling, J. Mann, and D. K. Arvind, "Respiratory rate and flow waveform estimation from tri-axial accelerometer data," in *Proc. Int. Conf. Body Sensor Netw.*, Jun. 2010, pp. 144–150.

[21] J.-W. Yoon, Y.-S. Noh, Y.-S. Kwon, W.-K. Kim, and H.-R. Yoon, "Improvement of dynamic respiration monitoring through sensor fusion of accelerometer and gyro-sensor," *J. Elect. Eng. Technol.*, vol. 9, no. 1, pp. 334–343, Jan. 2014, doi: 10.5370/JEET.2014.9.1.334.

[22] T. Elfaramawy, C. L. Fall, M. Morissette, F. Lellouche, and B. Gosselin, "Wireless respiratory monitoring and coughing detection using a wearable patch sensor network," in *Proc. 15th IEEE Int. New Circuits Syst. Conf. (NEWCAS)*, Jun. 2017, pp. 197–200.

[23] B. Ferdousi, S. M. F. Ahsanullah, K. Abdullah-Al-Mamun, and M. N. Huda, "Cough detection using speech analysis," in *Proc. 18th Int. Conf. Comput. Inf. Technol. (ICCIT)*, Dec. 2015, pp. 60–64.

Tamer Elfaramawy received the B.Sc. degree in electronics engineering, specialized in radio and telecommunication systems, from the Bordeaux Institute of Technology, Bordeaux, France, in 2014, and the M.Sc. degree in electrical engineering from Université Laval, Quebec, QC, Canada, in 2018. His project was the design of a respiratory and vital signs monitoring system. His main research interests are digital and analog circuit design, intelligent wireless biomedical sensors, and low-power body-implanted microsystems.

Cheikh Latyr Fall received the master's degree in automatic control and electrical engineering from the Institut National des Sciences Appliquées, Toulouse, France, in 2013. He is currently pursuing the Ph.D. degree in electrical engineering with the Biomedical Microsystems Laboratory, Laval University, Quebec, QC, Canada. His main research interests are assistive technologies, rehabilitation robotics, human–machine interfaces, wireless body sensor networks, and biomedical instrumentation.

Soodeh Arab received the B.Sc. degree in electrical engineering from Shariati University, Tehran, Iran, in 2006, the M.Sc. degree in opto-electronic engineering from the Shiraz University of Technology, Shiraz, Iran, in 2010, and her project was the design and simulation of a mixer for 2.4-GHZ communication standard using 0.18 μm CMOS technology, and the master's degree in bio-electrical engineering from Laval University in 2017, and her project was the implementing of a low-power wireless system for real-time health monitoring applications. In 2014, she started her research at Laval University as a Research Assistant. Her main research interests include design of analog CMOS integrated circuits (design, optimization, and modeling), RF microelectronics, wireless implantable biomedical systems, biomedical VLSI circuit design, wireless sensor interfaces, wireless power and data transmission, and circuit modeling/simulation/numerical analysis/computational techniques.

Martin Morissette received the bachelor's degree in electrical engineering. He has over 20 years of experience in research and development of innovative technologies in the telecommunications and medical devices sector. He is currently the Research and Development Director of OxyNov, a company specialized in the conception of medical devices for oxygen therapy.

François Lellouche received the M.D. degree in internal medicine in 2001 and critical care medicine in 2004 from the Pierre et Marie Curie University (Paris VI) and the Ph.D. degree in science and engineering: materials–modeling–environment from the University of Paris XII, under the supervision of Pr. L. Brochard. He was an INSERM–CIHR Post-Doctoral Fellow with the Saint-Michael Hospital Laboratory (Pr. Sinderby and A. Slutsky). He is currently a Critical Care Physician with the Quebec Heart and Lung University Institute and an Associate Professor with the Department of Medicine, Laval University. His research interests include humidification of gas during mechanical ventilation, noninvasive mechanical ventilation, high-flow oxygen therapy, and new modes of mechanical ventilation, focusing on automated modes of respiratory support and closed-loop oxygen supplementation.

He conducts at the research center of the Quebec Heart and Lung Institute bench studies, physiological studies focusing on breathing physiology and clinical trials to evaluate the clinical impact based on preliminary studies. His laboratory develops several innovative devices in the field of respiratory and oxygen support, including the FreeO_2 device, a new breakthrough closed-loop device that titrates oxygen flow based on patient's needs. He co-founded with Pr. E. L'Her the Oxynov company that manufactures and commercializes the FreeO_2 device.

Benoit Gosselin (S'02–M'08) received the Ph.D. degree in electrical engineering from the École Polytechnique de Montréal in 2009. In 2010, he was an NSERC Post-Doctoral Fellow with the Georgia Institute of Technology. He is currently an Associate Professor with the Department of ECE, Université Laval, where he is also leading the Biomedical Microsystems Laboratory. His research interests include wireless microsystems for brain–computer interfaces, analog-/mixed-mode and RF integrated circuits for neural engineering, interface circuits of implantable sensors/actuators, and point-of-care diagnostic microsystems for personalized healthcare.

Dr. Gosselin has received several awards, including the Mitacs Award for Outstanding Innovation and the NSERC Brockhouse Canada Prize for Interdisciplinary Research in Science and Engineering. He is currently the Chair and the Founder of the IEEE CAS/EMB Quebec Chapter (2015 Best New Chapter Award). He is also an Associate Editor of the IEEE TRANSACTIONS ON BIOMEDICAL CIRCUITS AND SYSTEMS. He served on the committees of several international conferences, such as IEEE BIOCAS, IEEE NEWCAS, IEEE EMBC, IEEE LSC, and IEEE ISCAS. His significant contribution to biomedical microsystems research led to the commercialization of the first wireless microelectronic platform for optogenetics and electrophysiology with live animals by Doric Lenses Inc.